

PRELIMINARY STUDY INTO THERMAL PROPERTIES OF CONTROLLED AXI-SYMMETRIC NOZZLE

S. Wawrzyniak, K. Peszyński*

Summary: *The paper presents the results of preliminary studies into thermal properties of controlled axi-symmetric nozzle. Downstream flow impinged on the 3.2 mm thick wall, with thermal scanner on the other side. Three types of downstream flow were studied: the first one of high velocity and a relatively small cross-section, the second one – an annular flow of big cross-section and low velocity, and the third one – switched in cycles between the above mentioned flows.*

Introduction

The paper presents the results of preliminary studies into thermal properties of controlled axi-symmetric nozzle. For the purpose of this research, a research stand has been developed, see Fig.1.

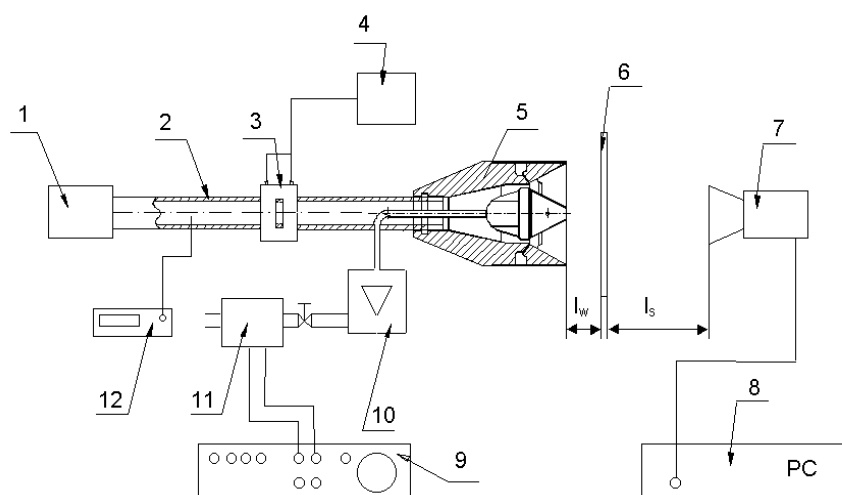


Fig. 1 Research stand diagram: 1 – fan with heater, 2- main pipe, 3 – orifice, 4 –micromanometer, 5 – nozzle, 6 – impinging wall, 7 – thermal camera, 8 – PC computer, 9 – frequency generator, 10 – rotameter, 11 – control flow valve, 12 – electronic main flow thermometer

* mgr inż. Sylwester Wawrzyniak, dr inż. Kazimierz Peszyński; University of Technology and Agriculture, Faculty of Mechanical Engineering, Department of Control and Machinery Design, ul. Kaliskiego 7, 85-796 Bydgoszcz, Poland

Research description

Nozzle output flow impinged on the 3.2 mm thick 0.42 m x 0.42 m wall, with thermal scanner on the other side Fig.1 – item 6. The wall was placed $l_w = 75$ mm away from the end of the nozzle. Such a distance between the wall and the nozzle results in the change in the flow direction on the wall when switching the jet from the first to the second state [Wawrzyniak S., 2002]. The wall temperature obtained was measured with thermographic camera, V-20 II type by VIGO System S.A. The camera is, in fact, a two-dimensional scanner which allows for obtaining the image of a maximum resolution of 240 x 240 pixels and thermal resolution of NETD 0.1°C. The camera was located 51 cm behind the wall. Such a distance between the camera and the wall surface allowed for examining the area of 0.39 m x 0.39m.

The camera may be connected to the PC with a serial port or USB (the present research use USB interface). THERM V-20 camera software stores measurement data and presents it as a default image whose pixels in respective colors stand for temperature of respective points of the object tested.



Fig. 2. Thermographic camera VIGO System S.A.

Three types of downstream flow were studied: the first one of high velocity and a relatively small cross-section, the second one – an annular flow of big cross-section and low velocity, and the third one – changed in cycles between the above mentioned flows. Jet switching occurred at the frequency 0.5, 1, 1.3, 2, and 3 Hz. The frequencies were selected following earlier paper [Wawrzyniak S., Peszyński K., 2003] in which the effect of the control flow frequency on absolute turbulence value in the nozzle output jet was studied..

A fan with heater (dryer) was used to generate the output jet of the flow intensity $Q_m = 0.0072126$ m³/s. The flow intensity in the supply pipe is calculated based on the pressure difference measured by the micromanometer (4) on the orifice (3).

The main jet reached the average temperature of $72.5 \div 73.0$ °C at maximum. The course of changes in the main temperature of the jet for each measurement cycle is presented in Fig 3.

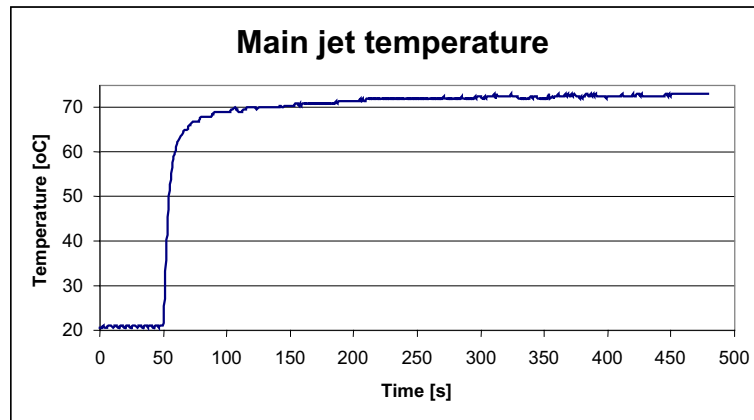


Fig. 3. Course of changes in temperature of the main jet for each measurement cycle

Each measurement cycle consists of 20 thermal scans, which takes 8 minutes. As mentioned above, the camera is, in fact, a two-dimensional scanner which allows for obtaining the image of a maximum resolution of 240×240 pixels, as used for the present measurements, over 25 seconds. The first 2 images were made without jet heating. The heating was switched on in the 50th second, which is visible on the graph in Fig. 3. To make the measurements results comparable, the research was carried out under the same initial conditions, namely the nozzle and wall temperature, which corresponded to the temperature $T_o = 22^\circ\text{C}$.

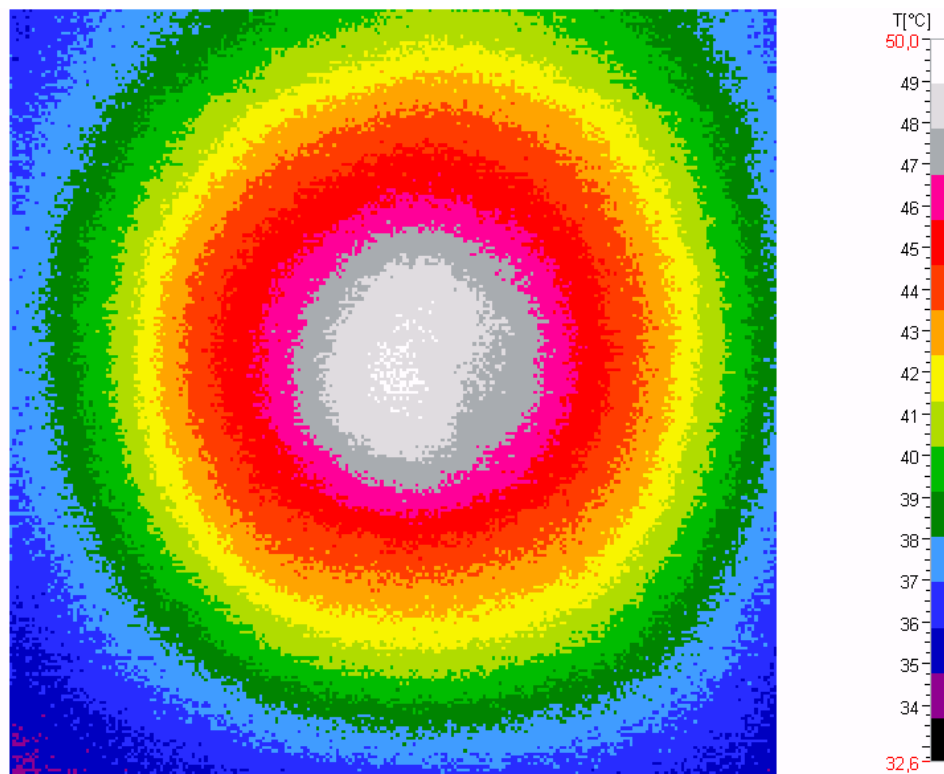


Fig. 4. Temperature distribution for the area tested for the jet in the first state (20th scan)

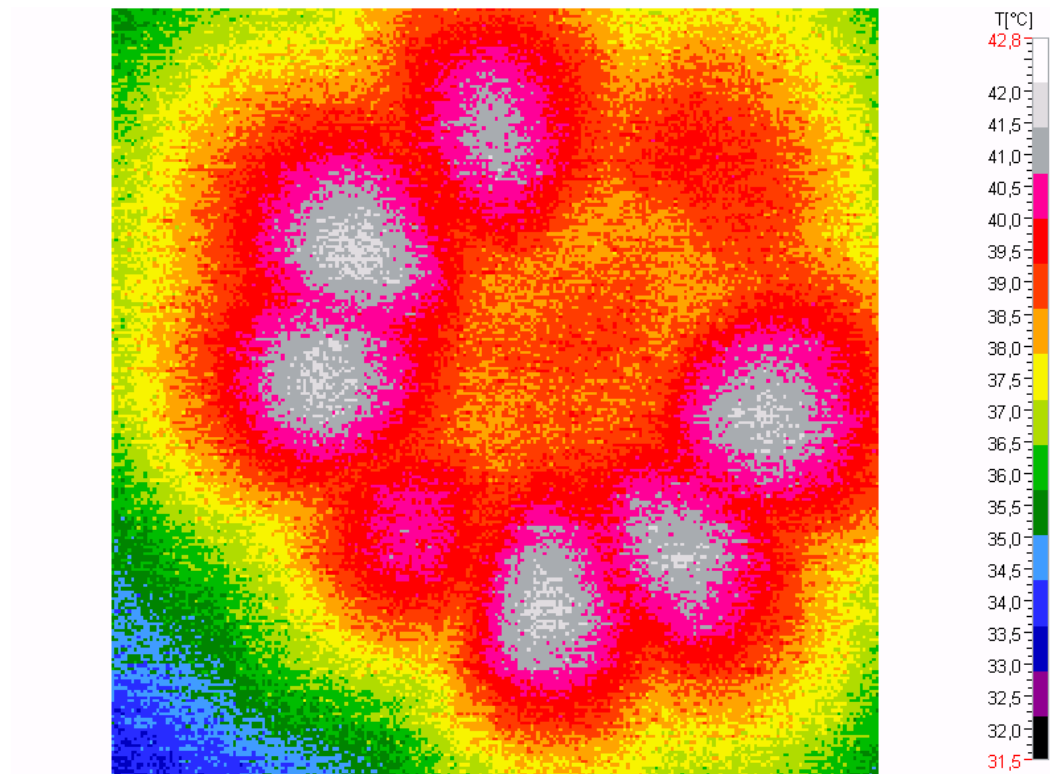


Fig. 5. Temperature distribution for the area tested for the jet in the second state (20th scan)

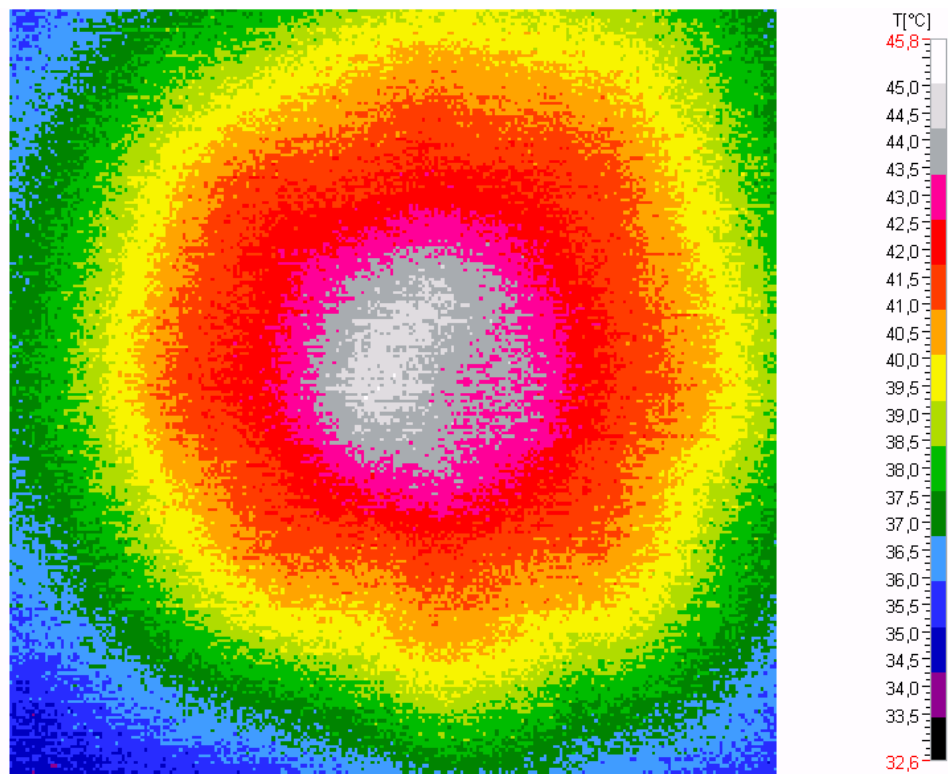


Fig. 6. Temperature distribution for the area tested for the jet being switched between the first and second state for frequency 1Hz (20th scan).

Selected images showing the temperature distribution for the area researched are given in Figs 4, 5, and 6. The greatest differences between the images selected were observed for the

maximum temperature for the first and second states. In the first state the maximum temperature was $T_{\max st1} = 49.29^{\circ}\text{C}$, in the second state – the maximum temperature of $T_{\max st2} = 41.99^{\circ}\text{C}$. For frequency 1 Hz, maximum temperature – $T_{\max 010\text{Hz}} = 44.96^{\circ}\text{C}$ was obtained. Table 1 presents a breakdown of wall temperatures for the 20th scan for the jet switching frequencies researched.

Table 1. Breakdown of wall temperatures for the control flow frequency researched.

	State 1	State 2	State 1-2 0.5Hz	State 1-2 1Hz	State 1-2 1.3Hz	State 1-2 2Hz	State 1-2 3Hz
Mean temperature	41.356	38.65	40.26	39.58	40.11	38.04	40.37
Mean square deviation	705364	142519.5	417478.19	286943.63	345497.49	320076.72	415359.4
Standard deviation	3.499	1.573	2.692	2.232	2.449	2.357	2.685
Max temperature	49.29	41.99	46.66	44.96	45.98	43.7	46.8
Min. temperature	34.29	33.14	33.70	34.01	34.28	32.11	34.63

The temperature distribution images obtained allow only for a qualitative evaluation of the effect of switching of the main jet by the control flow on the wall temperature. The temperature distribution image of the second state is of special interest (Fig.5). The radial distribution of the round spots shows the effect of the spoiler used, mounted on the external cone of the nozzle on 8 pins. It is the first such clear result showing the effect of spoiler pins on the output jet. In the earlier research of the output jet velocity and during the jet visualization the effect of spoiler pins was not observed.

The quantitative data, concerning the temperature of a given area, was exported to the text file and imported to Excel spreadsheet for numerical processing. Since each image contained information on 57,600 measured pixels in Visual Basic environment, subroutines were developed to accelerate the data processing considerably.

The figures below show a temperature distribution depending on the radius for the control flow frequencies researched and for the first and the second state.

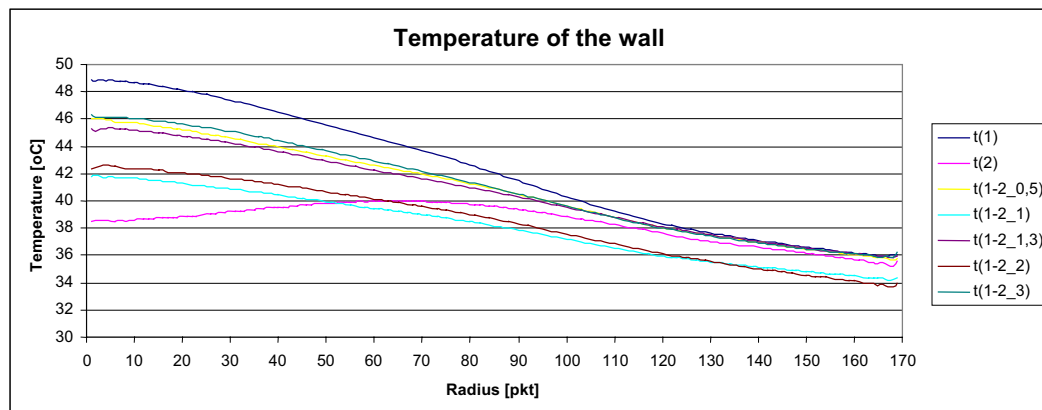


Fig. 7. Temperature distribution depending on the radius

For each radius, given in pixels, the mean temperature was calculated. Therefore point 0 in Fig. 7 stands for the center of the image (impinging jet axis), while point 170 – for the corners

of the image. While switching from the first to the second state the control flow of temperature $T_c = 22^\circ\text{C}$ and flow intensity $Q_c = 0,000861 \text{ m}^3 \cdot \text{s}^{-1}$ joins the hot main flow. As a result, the thermal properties of the main jet change. The results obtained were modified with a simplified coefficient of jet temperature change, factoring in a lower temperature of the control flow. The coefficient was calculated based on the thermal balance of air flows. When calculating the value of the coefficient, the main flow temperature was $T_m = 72^\circ\text{C}$ and the control flow temperature – $T_c = 22^\circ\text{C}$

Since the temperature of the main flow was measured, and the control involved air flow Q_c of the temperature of the environment accounting for 11.94% of the main flow intensity Q_m , the results of measurements have been distorted as the resultant jet was cooler. For that reason, a simplified linear correlation coefficient was applied c_k . The value of the coefficient in the second state was $c_k = 1,1$ while for states switched in cycles – $c_k = 1.05$.

Fig. 8 shows the temperature distribution of the area tested factoring in the temperature correction.

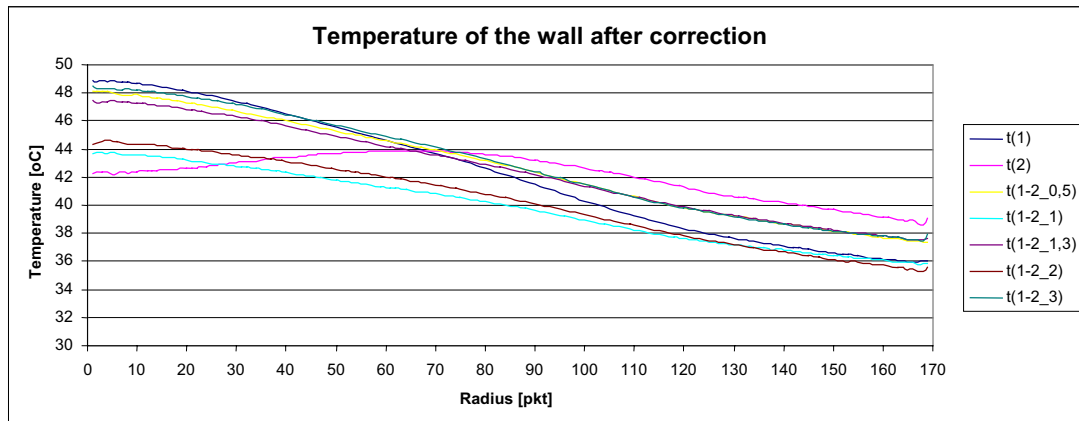


Fig. 8. Temperature distribution depending on the radius after correction for the 20th scan.

Fig. 9 presents the rate of temperature increase depending on the number of scan, which, in fact, means depending on time.

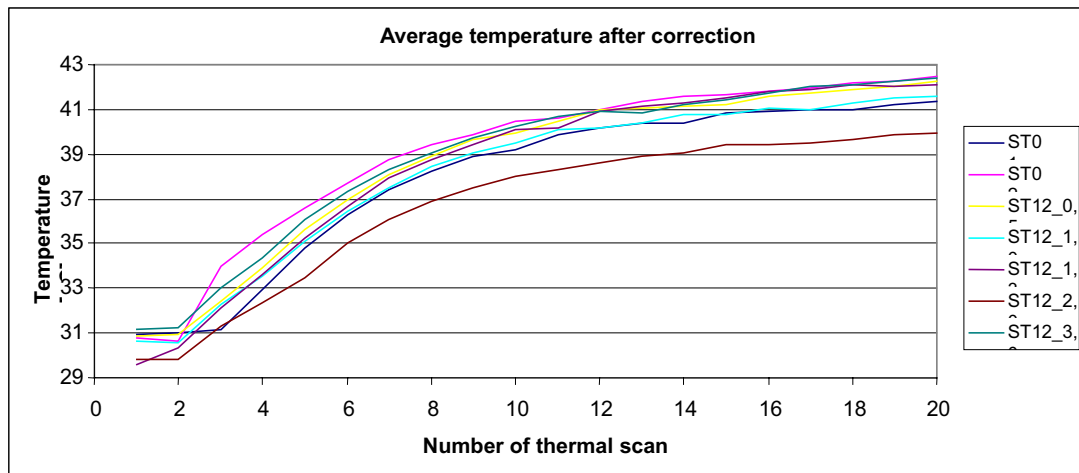


Fig. 9. Average wall temperature for successive scans

Conclusions

1. The results obtained clearly show that the maximum temperature can be recorded in the first state only. In that state also the greatest standard deviation was obtained, which points to most non-uniform temperature distribution on the area of the impinging wall researched. The lowest value of standard deviation, and so the most uniform temperature distribution, was recorded in the second state, however despite the continuous control flow, the minimum temperature was not the lowest.
2. Out of all the frequencies examined, 3 Hz was most favorable. For this frequency the highest mean temperature, the highest minimum and maximum temperature, but almost the highest value of standard deviation were obtained.
3. The results of the measurements given in Fig. 5 are very interesting. The analysis of nozzle conducted so far (i.e. numerical calculations with the use of Fluent solver) omitted the effect of spoiler pins on the output velocity. The most recent results show, however, that this assumption is unacceptable during detailed analyses. The problem must be considered at the next stage of research.

References

- Wawrzyniak S. (2002) 'Stanowisko do ciągłej wizualizacji przepływu w elementach strumieniowych' (in Polish) *VI conference 'Developments in Machinery Design and control – Bydgoszcz-Duszniki Zdrój October 03-05, 2002*, proceedings in a form of extended abstracts, p. 61, full text on CD-ROM
- Wawrzyniak S., Peszyński K. (2003) 'Continuous visualization of flow in power fluidic elements and basic analysis' National Conference with International Participation ENGINEERING MECHANICS 2003, Svratka, The Czech Republic
- Wawrzyniak S., Peszyński K. (2003) 'Investigations of turbulent pulsation changes and average velocity in axisymmetric nozzle in dependence on vibration damping forcing frequency' monograph in 'Developments in Machinery Design and Control Vol. 2' ATR University Press, collection of monographs in English, Bydgoszcz, 2003, p. 93-98